

# Mössbauer Spectroscopy

Evan Berkowitz

Junior, MIT Department of Physics

(Dated: April 19, 2007)

Using a Mössbauer drive and Michelson interferometer we perform an absolute velocity calibration, a calibration based on a Zeeman spectrum, and finally examine the effects of the isomer shift and quadrupole splitting. We find that the difference between  $\text{Fe}_2\text{O}_3$  and  $\text{Fe}_2(\text{SO}_4)_3$  due to isomer shift is  $0.11 \pm 0.04$  mm/s, the difference between  $\text{Fe}_2\text{O}_3$  and  $\text{Fe}_2\text{SO}_4 \cdot 7\text{H}_2\text{O}$  is  $0.909 \pm 0.018$  mm/s. Additionally, the quadrupole splitting of  $\text{Fe}_2\text{SO}_4 \cdot 7\text{H}_2\text{O}$  is measured to be  $3.38 \pm 0.16 \pm 0.07$  mm/s. These values are in good agreement with published values.

## 1. HISTORY AND PROBLEM STATEMENT

It is well understood from relativistic considerations that when a body gives off a photon, the photon carries momentum and thus the emitting body recoils. If  $E_\gamma$  is the energy of the emitted photon,  $m$  is the mass of the emitting body, and  $c$  is the speed of light, then the energy of the body gained  $E_{recoil}$  is given by

$$E_{recoil} = (mc^2 - E_\gamma) \left( 1 - \sqrt{1 - \frac{E_\gamma^2}{mc^2 - E_\gamma}} \right) \quad (1)$$

which, if  $E_\gamma \ll mc^2$ , may be Taylor expanded to first order, giving

$$E_{recoil} = \frac{1}{2} \frac{E_\gamma^2}{mc^2 - E_\gamma} \approx \frac{1}{2} \frac{E_\gamma^2}{mc^2} \quad (2)$$

This nonzero recoil makes it difficult to measure exactly frequency of the photon emitted in the lab frame, as it undergoes Doppler shift due to the moving source. Thus, high-precision measurements of emission lines becomes difficult.

However, in 1957 Rudolf Mössbauer discovered the effect which now bears his name. The idea Mössbauer had was this: what would happen if an emitting nucleus was embedded in a crystal? It turns out that due to the rigidity of crystal structure, it no longer seems as though only that nucleus was emitting the photon. Instead, Mössbauer found, recoilless emission occurred. If we replace  $m$  with the relatively large mass of the crystal  $M$  in (2) we conclude that  $E_{recoil}$  becomes extremely small. Thus, the effects which prevented high precision measurements before have become greatly diminished and the emitted photon has nearly all of the energy from the emission process. Mössbauer won the Nobel Prize in Physics only four years after his discovery.[1]

The revolution the Mössbauer Effect, as it is now known, was one of resolution. If  $E$  is the energy of the spectral line and  $\Delta E$  is the width of that line we define the resolution to be  $\frac{\Delta E}{E}$ . With other common experiments, it is reasonable to expect a resolution to be around  $10^2$  to  $10^4$ . Using Mössbauer spectroscopy, one

can achieve a resolution of  $10^{12}$  [2], revealing spectral details that would otherwise be inaccessible.

Mössbauer spectroscopy has quite a few uses: determining lifetimes of excited nuclear states, measuring nuclear magnetic moments, studying electric and magnetic fields in crystals, testing special relativity via the temperature-dependent motion of atoms. Famously, Pound and Rebka performed a measurement of gravitational redshift over the height of a small tower which conformed with the predictions of general relativity. [3]

In order to scan a spectrum of a sample, however, it is necessary to be able to vary the energy of the photons from the point of view of the sample, so that we may measure the different responses to different energies. With a recoilless emission the source produces photons of uniform energy. However, we may adjust the energy of the photons by moving the source with respect to the sample. Although we have just fought to remove an energy spread by embedding the source in a lattice, this energy shift is welcome because it can be controlled and measured by the experimenter. A schematic representation of this imposed energy change can be seen in FIG 1.

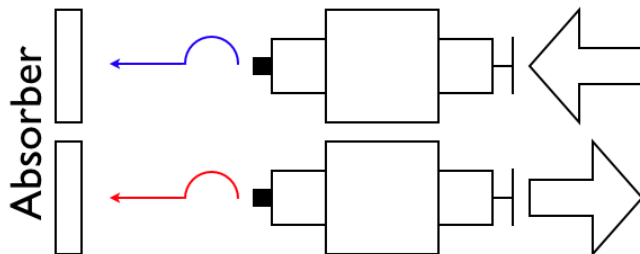


FIG. 1: By mounting the source on a moving piston we can change the energy of the emitted photon. When the piston moves towards the source, the photon gains energy and is blue-shifted. When the piston moves away from the source, the photon is appropriately red-shifted.

In these experiments, we mount an  $^{57}\text{Fe}$  source, which produces 14.4 keV nuclear emission lines [2], on a drive with variable speed to measure various features of the  $^{57}\text{Fe}$  spectrum when the nuclei are subject to a few different conditions.

## 2. EXPERIMENTAL APPARATUS

The primary apparatus of the experiment may be seen in FIG. 2. The source is composed of  $^{57}\text{Co}$  embedded in a platinum substrate.  $^{57}\text{Co}$  decays through electron capture into the second excited state (nuclear spin  $\frac{5}{2}$ ) of  $^{57}\text{Fe}$ . From this excited state, 91% of the nuclei decay to the first excited state (nuclear spin  $\frac{3}{2}$ ). The first excited state then decays to the ground state, giving off a 14.4 keV  $\gamma$ -ray. [2] All the other transitions differ in energy from 14.4 keV enough so that they do not appear in our spectra.

The SpecTech is a Multi-Channel Scaler (MCS) which provided a USB interface to the accompanying computer. Additionally, it controlled the drive circuit and received data from the signal chain which carried the information about the intensity received by the counter. If the counter registered a higher count (intensity), then the absorber was more easily penetrated. By correlating the intensity information with the drive information we could run many sweeps of the motion of the piston of the Mössbauer drive.

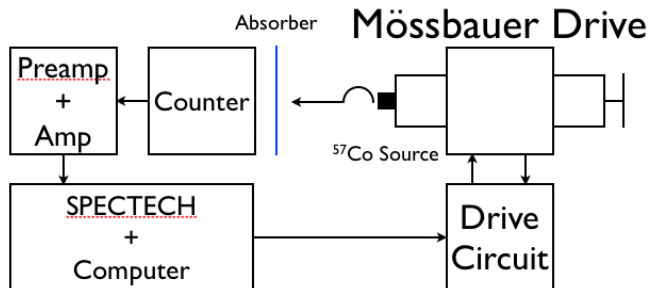


FIG. 2: The main workings of our experiments. The Mössbauer drive has a movable piston which is controlled by the SpecTech. This allows us to produce blue- and red-shift as shown in FIG. 1.

In order to do an absolute calibration of the Mössbauer drive's velocity, the apparatus discussed had an additional component. We used a Michelson interferometer, setup as shown in FIG. 3. The laser used was a Helium-Neon laser with a wavelength  $\lambda$  of 632.8 nm. The beam leaves the source and hits the beam splitter. Half the beam is redirected so as to hit a mirror attached to the moving piston on the Mössbauer drive, reflect towards the splitter, and pass into the photodiode. The other half passes directly to a mirror mounted opposite the laser, is reflected back to the splitter and towards the photodiode. By adjusting the beam splitter and then the mirror across from the laser we focused both beams directly onto the photodiode.

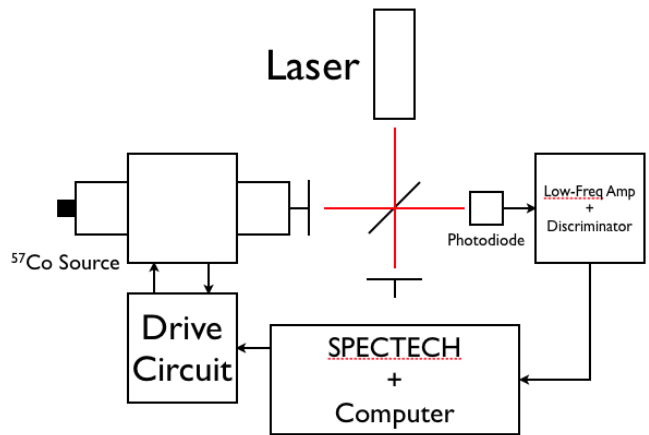


FIG. 3: The Michelson Interferometer used for absolute calibration.

The absolute calibration relies on the interference between the two beams. The part of the beam which does not hit the piston's mirror travels a static path to the photodiode. Conversely, the beam which hits the piston's mirror strikes travels a variable distance. When the two beams interfere constructively, the photodiode receives a strong signal and when they interfere destructively the photodiode receives no signal. Since the other beam is static, when the mirror on the piston moves one wavelength the photodiode will see an entire constructive-destructive cycle. The photodiode passes its signal to the SpecTech, which bins the counts according to their time value. If  $C_i$  is the number of counts in the  $i^{\text{th}}$  bin,  $\lambda$  the wavelength of the laser,  $N$  the number of passes the piston makes, and  $T$  the time interval for each bin, the velocity at the  $i^{\text{th}}$  bin  $V_i$  is given by

$$V_i = \frac{C_i \lambda}{2NT} \quad (3)$$

A typical calibration is shown in Figure 4. The unusual feature at the beginning of the curve is due to the jerk the piston experiences: the piston is driven by a sawtooth current, and when the current resets we see the sharp dip. Where the curve is zero the piston must be still.

By fitting straight lines to those curves, we find that each bin in time (0.2 ms) corresponds to a change of velocity  $\Delta V$  of  $0.0214 \pm 0.004$  mm/s. Additionally, there is a more practical and convenient calibration possible, which requires the use of a  $^{57}\text{Fe}$  spectrum.

## 3. ZEEMAN SPLITTING CALIBRATION

Metallic iron has an internal magnetic field, which separates the energy-degenerate states of the  $^{57}\text{Fe}$  nucleus into separate energy levels. Under the magnetic field influence, the ground state (spin  $\frac{1}{2}$ ) splits into two and the first excited state (spin  $\frac{3}{2}$ ) splits into four, as described in

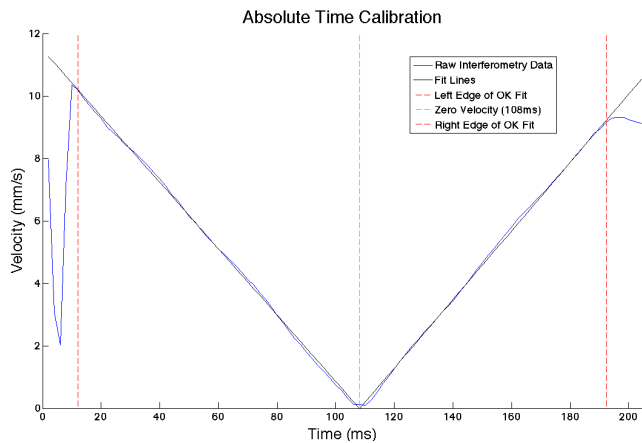


FIG. 4: The small oscillations of the actual data around the best fit curves are a result of inexact tuning and noise. Any time left of the zero velocity (108 ms) has a negative velocity and any time to the right of that turning point has a positive velocity.

detail in [4]. These splittings and the allowed transitions between the nondegenerate states are shown in FIG 5.

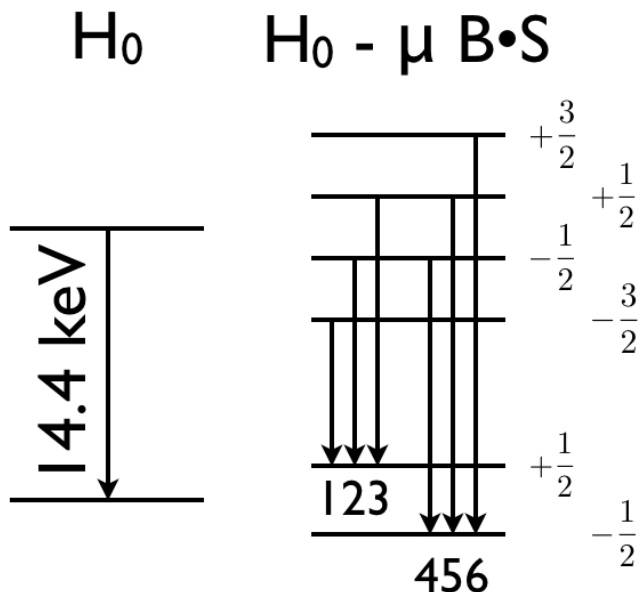


FIG. 5: A figure comparing the no-magnetic-field case to the case with magnetic field. The six allowed transitions between the nondegenerate states are shown, with the splitting exaggerated for clarity.  $H_0$  represents the standard Hamiltonian, and  $H_0 - \mu B \cdot S$  represents the Hamiltonian with the magnetic field perturbation.

Using known values for the separations of a nuclear Zeeman split in  $^{57}\text{Fe}$ , we can use a  $^{57}\text{Fe}$  spectrum as a secondary calibration. One typical enriched metallic  $^{57}\text{Fe}$  spectrum is shown in FIG. 6

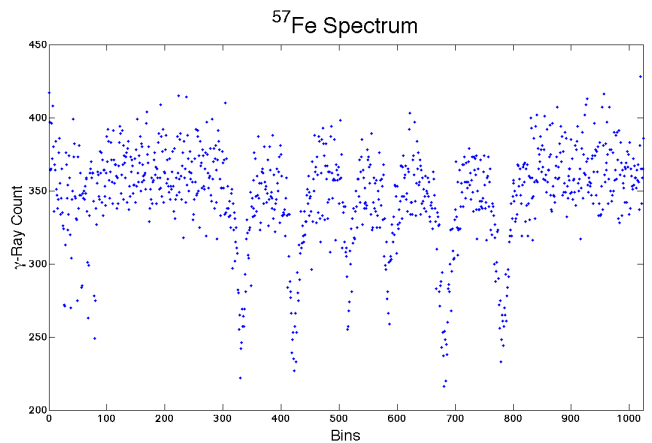


FIG. 6: A typical enriched metallic  $^{57}\text{Fe}$  spectrum. All six transitions are apparent. The  $x$ -axis is labeled in bins to emphasize that we are calibrating that axis. The 1024  $x$ -axis bins correspond linearly to 205 ms.

From this calibration, we find that the change in velocity per bin  $\Delta V$  is  $0.0234 \pm 0.004$  mm/s. We account for the discrepancy between the two calibrations in three ways. First, the Zeeman splittings are extremely sensitive to magnetic fields. If the sample were in even a small field which was against the internal field, this would push the lines closer, meaning that the velocity differences would be accounted for in fewer bins, leading to a higher  $\Delta V$ . Secondly, the splittings are temperature sensitive, and although the known velocities are at a temperature similar to the one in which we did the experiment, it is possible that a small difference might occur. We expect this effect to be too small to account for the large difference.

Finally, if we allow for loss in our interferometer signal chain, we find what could be a significant factor in the discrepancy. Suppose some fraction of all pulses picked up by the photodiode did not get counted. This would cause the  $v$ -shape to broaden yet remain linear, as bins with a higher speed correspond to more pulses and thus more pulses lost. If this occurred, the counts in each bin would decrease, thus lowering the perceived velocity as well, leading to a deceptively low  $\Delta V$ . To account for the whole difference, the circuit would have to lose 8.55% of the photons. This seems to be unreasonably high, and so this effect cannot possibly be the only source of the discrepancy, but it can certainly contribute.

#### 4. ISOMER SHIFT AND QUADRUPOLE SPLITTING

The electrons and nuclei in an atom interact electromagnetically. This interaction depends slightly upon the electron density at the nucleus. If the emitting  $^{57}\text{Fe}$  is in a different electromagnetic environment than the absorbing  $^{57}\text{Fe}$ , the resonances will differ. Using old terminology, an excited nuclear state or “isomer” exhibits

a different resonance dependent upon its environment, leading to this effect. If there is a greater electron density at the absorber than the emitter, the absorber will require more energy than 14.4 keV to transition, and thus the lines will shift to the right.[2]

Electric quadrupole splitting occurs when a nucleus with a quadrupole moment is exposed to an electric field gradient. In a similar way as a magnetic field distinguishes a magnetic moment into states where the spin is either parallel or antiparallel to the field, the electric field gradient distinguishes the excited states resulting in two possible energy transitions.

The composition of these effects can be seen in FIG. 7 Using an  $\text{Fe}_2\text{O}_3$  spectrum as a velocity calibration as discussed in Section 3, we examine additionally an  $\text{Fe}_2(\text{SO}_4)_3$  spectrum and an  $\text{FeSO}_4$  spectrum. Calibrating against the Zeeman splitting data for  $\text{Fe}_2\text{O}_3$  [5], we find a  $\Delta V$  of  $0.0276 \pm 0.0009$  mm/s. As the centers of the  $\text{Fe}_2\text{O}_3$  and  $\text{Fe}_2(\text{SO}_4)_3$  are four bins apart, we find a difference of  $0.11 \pm 0.04$  mm/s. This agrees well with the difference published by DeBenedetti et al. of 0.14 mm/s.[6] When comparing the  $\text{Fe}_2\text{SO}_4 \cdot 7\text{H}_2\text{O}$  spectrum to the  $\text{Fe}_2\text{O}_3$ , we find that their centers are 33 bins apart, or  $0.909 \pm 0.018$  mm/s, agreeing well with the published value of  $0.90 \pm 0.05$  mm/s.[6]

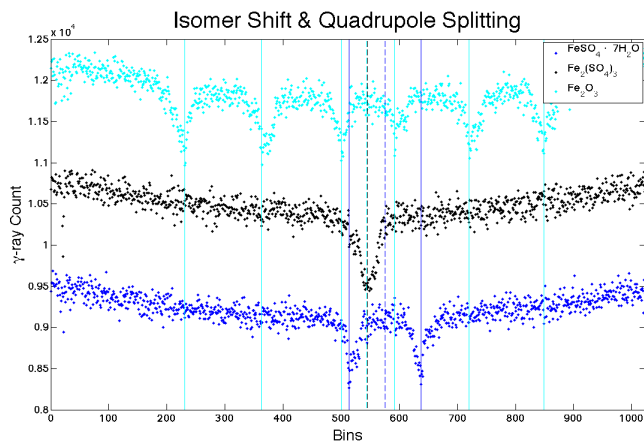


FIG. 7: The Zeeman spectrum of  $\text{Fe}_2\text{O}_3$  (cyan) is used to calibrate the bins (1024 bins for 205 ms) in terms of velocity. The solid vertical lines indicate the used values for the corresponding peaks, and the dashed vertical lines indicate the average value of these peaks. Note that the cyan and black dashed lines are only four bins apart, yet at this resolution they appear to be in consecutive bins.

Finally, we find the distance between the minima in the absorption lines of the  $\text{Fe}_2\text{SO}_4 \cdot 7\text{H}_2\text{O}$  is  $123 \pm 6$  bins, or  $3.38 \pm 0.16 \pm 0.07$  mm/s, where the first uncertainty comes from the uncertainty in bins and the second from the uncertainty in the calibration. These values agree very well with the published value of  $3.2 \pm 0.05$  mm/s.[6]

## 5. CONCLUSIONS

We have demonstrated the technique of nuclear spectroscopy via the Mössbauer effect, yielding a resolution sharp enough to see interesting features in detailed spectra by controlling the energy of a recoilless emission. By using a Michelson interferometer we have calibrated our energy scale exactly and have found that alternatively calibrating against a Zeeman splitting gives relatively reliable numbers, though our two distinct calibrations do not agree. When calibrating against the Zeeman splitting in  $\text{Fe}_2\text{O}_3$  and without bothering to do an absolute calibration, we found with excellent agreement with published values, the difference in isomer shift between  $\text{Fe}_2\text{O}_3$  and  $\text{Fe}_2(\text{SO}_4)_3$  to be  $0.11 \pm 0.04$  mm/s, the difference in isomer shift between  $\text{Fe}_2\text{O}_3$  and  $\text{Fe}_2\text{SO}_4 \cdot 7\text{H}_2\text{O}$  to be  $0.909 \pm 0.018$  mm/s, and the quadrupole splitting of  $\text{Fe}_2\text{SO}_4 \cdot 7\text{H}_2\text{O}$  to be  $3.38 \pm 0.16 \pm 0.07$  at room temperature.

- [1] *Recoilless nuclear resonance absorption of gamma radiation* (Rudolf Mössbauer for The Nobel Foundation, 1961).
- [2] J. L. Staff, *Mössbauer spectroscopy*, <http://web.mit.edu/8.13/www/JLEperiments/JLExp13.pdf> (2007).
- [3] M. Tegmark (2005), 8.033 Class Lecture - Evidence For General Relativity.
- [4] C. Cohen-Tannoudji, *Quantum Mechanics* (John Wiley & Sons, 2005), vol. Two, chap. Complement D XII, pp.

1271–1278.

- [5] A. S. Associates, *S-700A Mossbauer Spectrometer Drive Module*, <https://web.mit.edu/8.13/8.13d/manuals/mossbauer-asa-s700a-drive-motor.pdf> ed. (????).
- [6] S. DeBenedetti, G. Lang, and R. Ingalls, *Phys. Rev. Lett.* **6**, 60 (1961).